UNCONVENTIONAL RESOURCES TECHNOLOGY CONFERENCE
FUELED BY SPE • AAPG • SEG

Notice: This material may be protected by copyright law (Title 17 U. S. Code).

URTeC: 5241

Analysis and Integration of the Hydraulic Fracturing Test Site-2 (HFTS-2) Comprehensive Dataset

Venkateswaran Sriram Pudugramam*, Yu Zhao, Fadila Bessa, Jake Li, Nancy Zakhour, Tim Brown, Jichao Han, Iwan Harmawan, and Vinay Sahni, Occidental

Copyright 2021, Unconventional Resources Technology Conference (URTeC) DOI 10.15530/urtec-2021-5241

This paper was prepared for presentation at the Unconventional Resources Technology Conference held in Houston, Texas, USA, 26-28 July 2021.

The URTeC Technical Program Committee accepted this presentation on the basis of information contained in an abstract submitted by the author(s). The contents of this paper have not been reviewed by URTeC and URTeC does not warrant the accuracy, reliability, or timeliness of any information herein. All information is the responsibility of, and, is subject to corrections by the author(s). Any person or entity that relies on any information obtained from this paper does so at their own risk. The information herein does not necessarily reflect any position of URTeC. Any reproduction, distribution, or storage of any part of this paper by anyone other than the author without the written consent of URTeC is prohibited.

Abstract

Objectives/Scope: Hydraulic Fracturing Test Site-2 (HFTS-2) is a field-based research experiment performed in the Permian (Delaware) Basin. The unique aspect of this program was the acquisition of a unique, comprehensive, diagnostic dataset. Additionally, shorter parent wells drilled three years before the child wells offered clear distinction between the stages influenced by parent-child effects and the stages without any effects. The goal of this study was to analyze and integrate this comprehensive diagnostic dataset to understand the areal and vertical extent of hydraulic fractures (HF). The paper also provides insights on the effects of parent wells' depletion on child well HF geometry based on various monitoring methods and subsurface models.

Methods, Procedures, Process: Areal and vertical coverage for all HFTS-2 wells during stimulation and depletion was estimated based on analysis and interpretation of diagnostics and advanced modeling results. HFTS-2 diagnostics included microseismic (MS), pre- and post-stimulation logs and cores, bottomhole gauges, and fiber optic (FO) data. The diagnostics results (MS, FO, image logs) were integrated and used to calibrate subsurface models. Additional field tests were designed and implemented for depletion monitoring. The tailored program for monitoring depletion included vertical and slant well pressures, interference testing, and a vertical strain depletion trial.

Results, Observations, Conclusions:

Areal Coverage: Conventional MS (and FO MS) were used to compute HF dimensions, which were compared with diagnostics (FO strain, gauge, image logs) observations and calibrated subsurface models. A post-production interference test did not show offset well communication.

Vertical Coverage: Vertical coverage during stimulation was monitored using a vertical monitoring well. The stronger mechanical strain signals showed good correlation with MS event intensities, geomechanical properties, and gauge inferences. Vertical depletion was estimated based on vertical/slant well gauges and strain depletion tests.

Parent-Child Effects: Diagnostics and calibrated subsurface models show asymmetry in child well fracture geometries for stages that overlap parent wells. Child well image logs serve as a good indicator for parent

Downloaded from http://onepetro.org/URTECONF/proceedings-pdf/21URTC/2-21URTC/D021S031R004/2477423/urtec-2021-5241-ms.pdf/1 by Carol Worster on 28 February 2022

well HF tracking. Child well MS events had an eastward bias, in line with pre-stimulation image logs, and was confirmed by parent well frac hits.

Novel/Additive Information: The dataset presents a unique, over-constrained problem space to compare independent techniques to arrive at HF metrics (i.e., stimulation height and/or half-length), unlike a single-source dataset, in which calibration is done using available data to guide predictions. The asymmetry in HF geometry seen in the stages influenced by parent-child effects offers unique insights into well spacing and landing, which are key capital decisions the unconventional resources industry is seeking to optimize.

Downloaded from http://onepetro.org/URTECONF/proceedings-pdf/21URTC/2-21URTC/D021S031R004/2477423/urtec-2021-5241-ms.pdf/1 by Carol Worster on 28 February 2022

Introduction and Objectives

The Hydraulic Fracture Test Site-2 (HFTS-2) is a cost-shared, field-scale R&D program in the Permian (Delaware) Basin. Occidental is the host and operator of this program with 18 consortia members. The dataset acquired in the program included microseismic (MS), 1,500 ft of whole core including 1,000 ft of SRV core, DFIT, PVT, Quad Combo and image logs, proppant logs, geochemical data, 28 bottomhole gauges' P/T data in production and science wells, varying completions, and fiber optic cable in two horizontal wells and one vertical well. The unique aspects of the program are the one-of-a-kind, comprehensive dataset and the application and demonstration of fiber optic (FO) technology for stimulation and production monitoring and fracture diagnostics. The two horizontal parent wells, drilled 3 years prior, are shorter than the four child wells, thereby offering a clear distinction between the stages influenced by parent-child effects and the stages without any depletion effects. The asymmetry in fracture geometry, which influences well spacing and landing decisions, is a critical piece of the puzzle to optimize capital expenditure and reduce the environmental footprint of the unconventional resources industry.

Project Area

The Hydraulic Fracture Test Site-2 (HFTS-2) is in the Delaware Basin about 140 miles west of the HFTS-1 project area (Figure 1). The HFTS-2 project area includes two parent horizontal wells (BR1H and BR2H) drilled and completed three years before the child wells, four horizontal Boxwood wells (BX1H, BX2H, BX3H, and BX4H) spanning the Wolfcamp-X to Wolfcamp-A formations. The average lateral length of the parent wells is 60% of the four child wells, so a portion of the lateral length on the child wells was affected by depletion. The project area also includes a vertical well (B5PH) drilled before the child well stimulation, and one slant core well (B6S) drilled after the child well stimulation, covering up to the Wolfcamp-B bench. The vertical well (B5PH) also had fiber optic cable installed, as did two adjacent horizontal wells (BX3H and BX4H). The setup and interpretation of near-wellbore DAS/DTS data is covered in detail in another paper (Zakhour et al., 2021).

There are 8 bottomhole gauges on the vertical well (B5PH) and 12 bottomhole gauges on the slant well (B6S). About 500 ft of whole core was recovered from the vertical well (B5PH) prior to the hydraulic fracturing of the child wells. About 1,000 ft of SRV core was recovered from the slant core well (B6S) after the child wells were fractured. The child horizontal wells have a rich dataset that includes heel and toe P/T gauges, Quad Combo and image logs, geochemical data, DFIT and PVT on two wells, and a proppant log on one well. There are conventional microseismic (MS) data on two wells in addition to FO-based MS data. The completion design, which varied in stage design, proppant, and fluid loading along and between the wells, is covered in detail in Zakhour et al., 2021. The child horizontal wells are spaced at ~700 ft with about 250 ft in vertical variation. See Figure 2 for a schematic of the wells.

Looking at the project area from the top view, we can separate the project area into a North sector and a South sector. The South sector includes the parent wells where depletion or parent-child effects come into play, and the North sector, which has the vertical well (B5PH) and the slant core well (B6S), will have no depletion effects. See Figure 2 for a delineation of the North and South sectors.

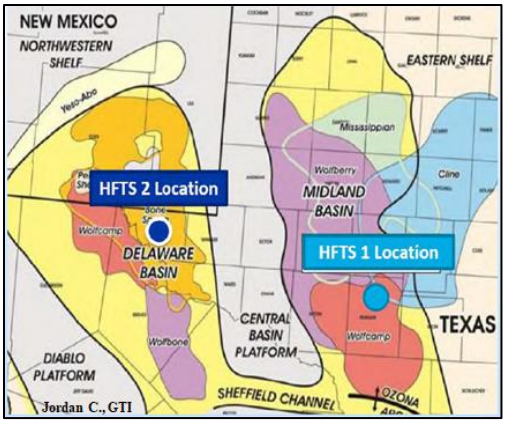

Figure 1. Location of the HFTS-2 project area

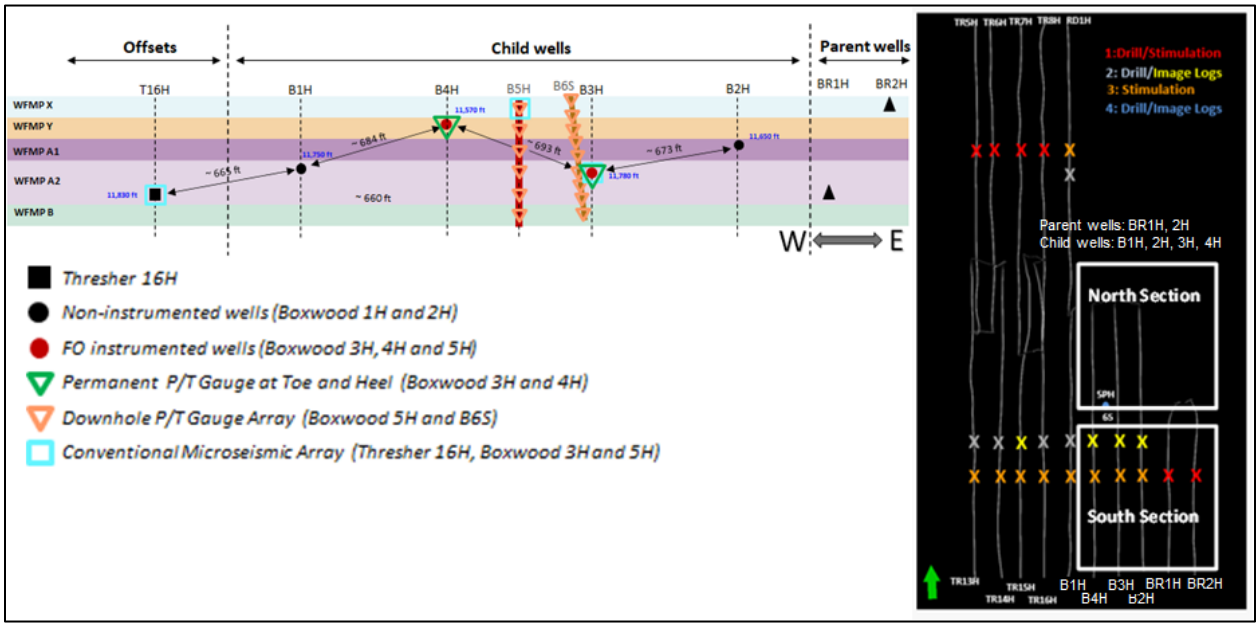

Figure 2. Left: Schematic of the HFTS-2 wells (gun barrel view); Right: Delineation of the North and South sectors (plan view)

HFTS-2 Dataset

Microseismic Data

A full description of the microseismic acquisition and processing is provided in Grechka et al., 2021. The objective of the microseismic acquisition is to estimate SRV and integrate observations with other diagnostic techniques to understand well and reservoir interactions better. The primary observations include:

- Eastward growth of events during the BX1H and BX2H stimulations toward the BR1H and BR2H due to reactivation in overlapping stages (Figure 3);
- Limited horizontal growth of seismicity for the BX1H and eastward growth for the BX2H stages north of the BR1H and BR2H overlap (Figure 4);
- Additional horizontal asymmetry for the BX2H and BX4H due to sequential ordering of completions; and
- Majority of seismicity is vertically constrained from top of Wolfcamp to Wolfcamp-B.

Downloaded from http://onepetro.org/URTECONF/proceedings-pdf/21URTC/2-21URTC/D021S031R004/2477423/urtec-2021-5241-ms.pdf/1 by Carol Worster on 28 February 2022

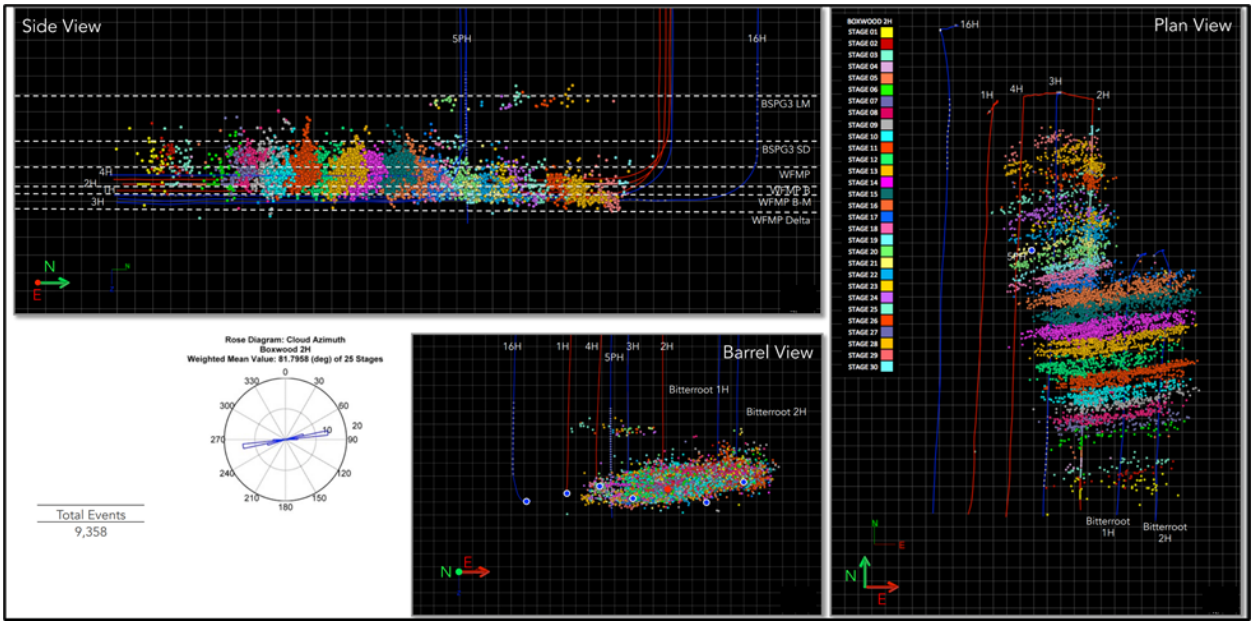

Figure 3. Microseismic display of high-quality events from the BX2H completion. The gun-barrel and plan views demonstrate the eastward growth in the area overlapping the Bitterroot wells.

Figure 4 shows a split comparison of the stages of BX1H affected by depletion and the stages without any depletion effects. Most of the microseismic events (failures) are within the lowest effective stress zone (violet zone), and the non-depleted stages show a more confined event distribution.

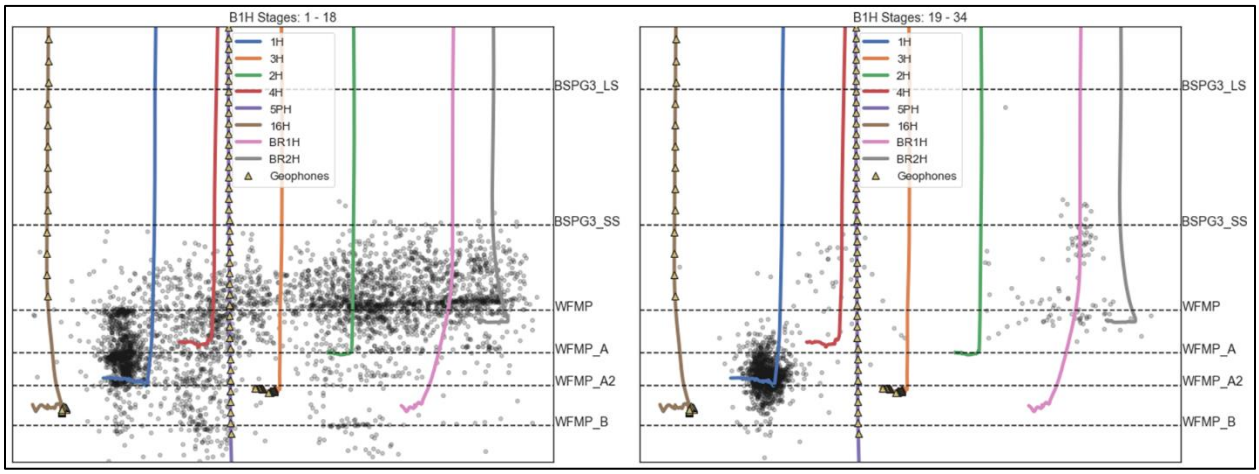

Figure 4. Split comparison of microseismic events for stages in the depleted (Left) and non-depleted (Right) zones.

The DAS microseismic was not used for SRV estimates because events were mapped using a single plane solution, which does not yield accurate 3D locations. However, the seismic deformation was compared to the aseismic deformation recorded by the low-frequency DAS. As seen in Figure 5, the dynamic vertical growth of the microseismic lags compared to the strain response on the low-frequency DAS, which demonstrates that the hydraulic fracture front is generally aseismic.

Downloaded from http://onepetro.org/URTECONF/proceedings-pdf/21URTC/2-21URTC/D021S031R004/2477423/urtec-2021-5241-ms.pdf/1 by Carol Worster on 28 February 2022

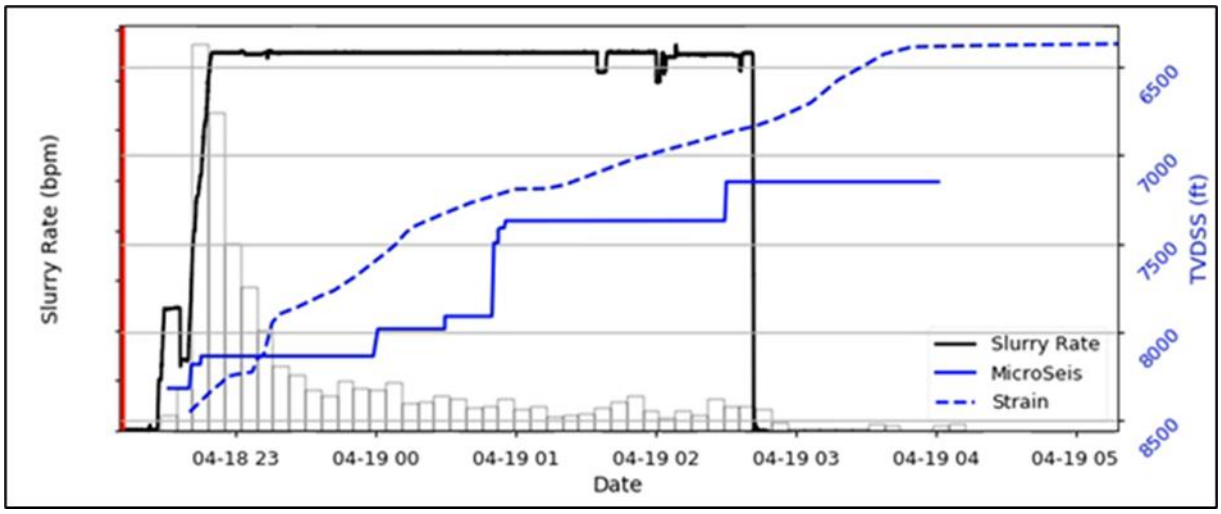

Figure 5. Dynamic upward growth of the microseismic (solid blue) vs. strain signal recorded by the low-frequency DAS (dashed blue). The microseismic lags the strain response.

Pre- and Post-Stimulation Logs and Core Data

The highlights of the stimulation logs and core interpretation as related to the integration with other datasets are covered in this section; the details are covered in Bessa et al., 2021. The SRV core obtained from the slant well (B6S) showed that the hydraulic fracture was planar and the orientation for Shmax was around 80°, which was confirmed by microseismic data, fiber optic data, and a regional sonic azimuthal anisotropy study. The image logs on BX2H, which were obtained before stimulation of the child wells but after the parent wells' stimulation, also show two distinct fracture sets: NE-SW oriented resistive fractures, and hydraulic-induced conductive fractures oriented around 80°. The intensity of conductive fractures along the lateral length of BX2H showed an interesting trend separating the North and the South sectors. The South sector, affected by the parent wells' stimulation, saw a higher intensity of conductive fractures, as shown in Figure 6. This observation was corroborated by the GTI proprietary proppant analysis, which measured the count of proppant in the mud log samples along the lateral length.

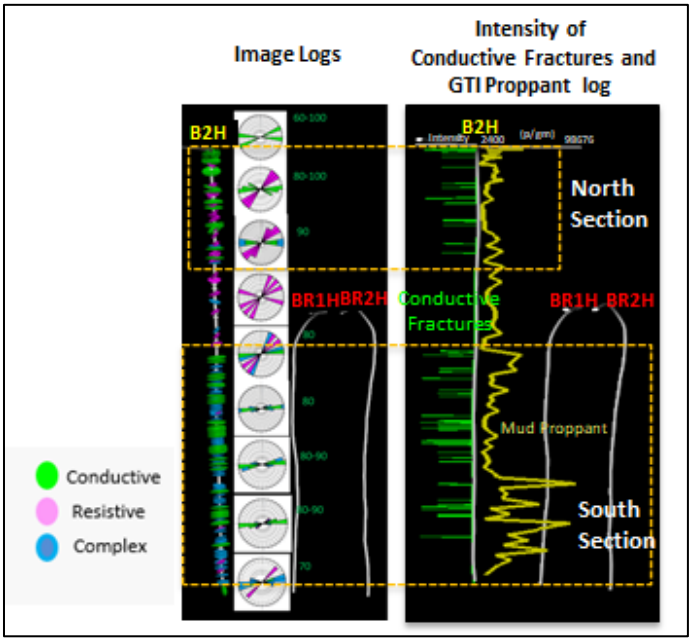

Figure 6. Image and GTI proprietary proppant logs in the North and South sectors

Downloaded from http://onepetro.org/URTECONF/proceedings-pdf/21URTC/2-21URTC/D021S031R004/2477423/urtec-2021-5241-ms.pdf/1 by Carol Worster on 28 February 2022

Fiber Optic Data

In the HFTS-2 project area, fiber optic cable was permanently installed in two horizontal child wells (BX3H, BX4H) and one vertical well (B5PH). This unique three-well design enables spatial and temporal HF propagation and production depletion monitoring. There are two kinds of data obtained from this fiber: near-wellbore survey and far-field survey. The near-wellbore survey measures the response from the activity in the fiber wells, whereas the far-field survey measures the response from the activity in the offset wells. In the near-wellbore survey, Distributed Acoustic Sensing (DAS) and Distributed Temperature Sensing (DTS) data were acquired during stimulation of the two horizontal fiber wells. These data were used to quantify pumped fluid/proppant allocation among the clusters and evaluate stimulation efficiency for different completion designs. During the production phase, Distributed Strain Sensing - Rayleigh Frequency Shift (DSS-RFS) (Jin et al., 2021, Ugueto et al., 2021) data were acquired in the near-wellbore region, which allowed us to gain insights on time-dependent fracture property changes. The integrated analysis and interpretation of the near-wellbore survey data are covered in detail in Zakhour et al., 2021.

Through the far-field survey, cross-well strain rate data were obtained by the low-frequency DAS technique from all three fiber wells and integrated with other diagnostics to achieve a better understanding of spatial and temporal characteristics of hydraulic fracture propagation (Molenaar and Cox, 2013; Jin and Roy, 2017; Ugueto et al., 2019). Figure 7 shows a typical example of cross-well strain acquired on the BX3H well during the treatment of Stage 3 on BX4H consisting of 6 clusters, 24 perforation holes, and 32-ft perforation cluster spacing. With the start of the stage injection, the emerging cone-shaped red strain rate signals indicate the propagation of hydraulic fractures from BX4H to BX3H, and 5 frac hits were indicated by yellow stars, where there is significant tensile deformation while the surrounding rocks are being compressed simultaneously. Figure 7 also clearly shows that the lateral coverage (248 ft) of frac hits on BX3H is almost the same as the stimulated stage length (250 ft) on BX4H. This observation is common to all treatment stages on the BX1H, BX2H, and BX4H wells, which indicates planar fracture propagation in the formation. As stated in the previous section, the Shmax orientation is suggested to be around 80° through integrated data analysis from multiple diagnostics (i.e., FO, MS, image logs, and SRV core).

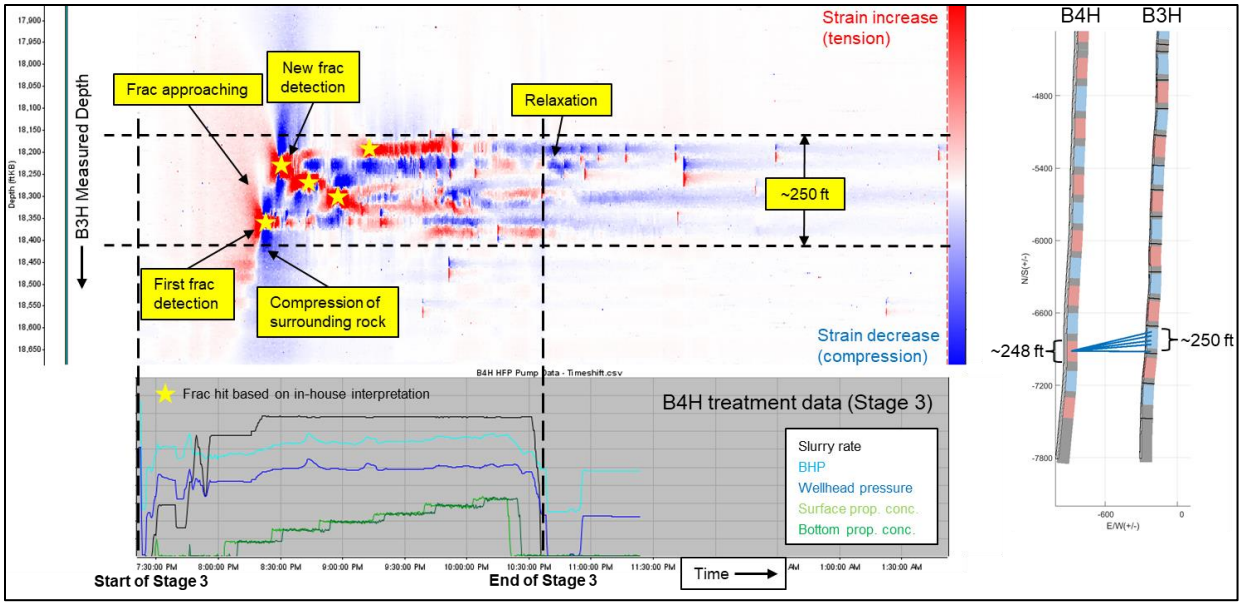

Figure 7. Far-field cross-well strain data acquired on BX3H during the treatment of Stage 3 (6×24) on BX4H

Figure 8 shows the frac hits detected on the BX3H and BX4H wells during the treatment of BX1H and BX2H. The blue bars represent the cluster number of each treatment stage, while the orange and green bars represent the number of detected frac hits from vendor and in-house interpretations. For the BX1H well, which was the first well stimulated in the pad, BX4H detected more frac hits than did the BX3H well due

Downloaded from http://onepetro.org/URTECONF/proceedings-pdf/21URTC/2-21URTC/D021S031R004/2477423/urtec-2021-5241-ms.pdf/1 by Carol Worster on 28 February 2022

to its proximity to BX1H. During the treatment of BX2H, more frac hits were also detected on BX4H than on the BX3H well, although BX3H is closer to BX2H horizontally. This observation can be explained by the shorter vertical distance between BX2H and BX4H, which also implies the upward growth trend of the hydraulic fractures. The relatively small number of detected frac hits on BX3H for Stages 1–17 on the BX2H well indicates a clear eastward growth preference for the BX2H stages that overlap with the two parent wells due to the production depletion effect.

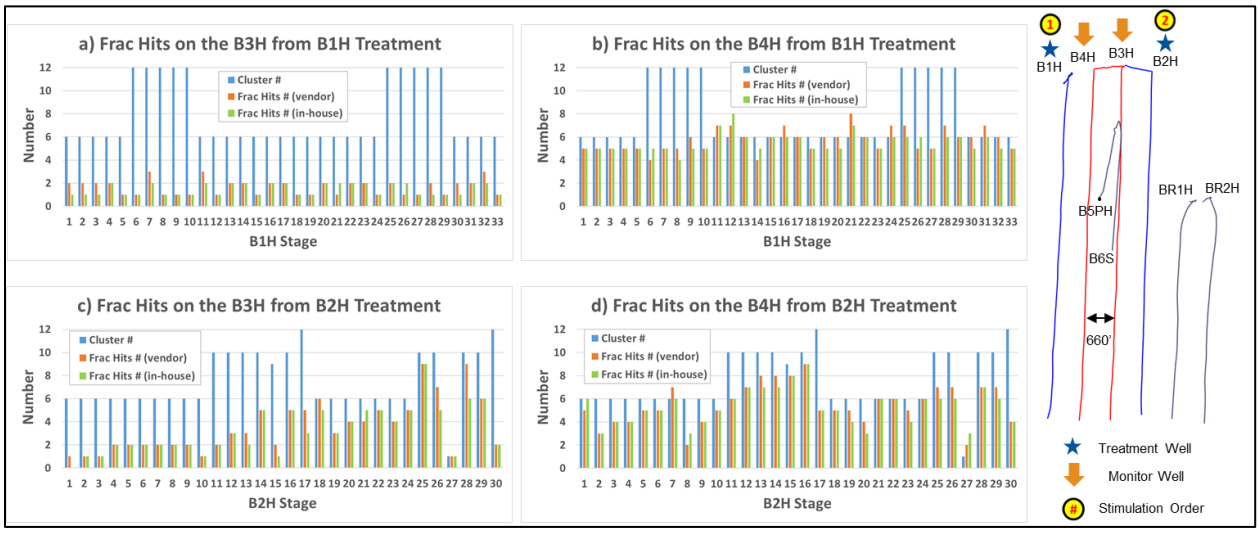

Figure 8. Frac hits on the BX3H and BX4H wells during the treatment of BX1H and BX2H.

During the treatment of the child wells (BX1H-BX4H), far-field cross-well strain data were also acquired in the vertical fiber well, B5PH, which offered a great opportunity to gain better understanding of vertical propagation and height of hydraulic fractures. Figure 9 shows the strongest cross-well strain data acquired on the B5PH during the treatment of two stages on the BX1H and BX4H wells. FO is very sensitive to small strain changes, and for that reason the strongest strain signals on B5PH could cover from 2nd Bone Spring to Wolfcamp-B, and the total height of strain signals is as large as ~2,000 ft. However, the strain signals in the black-circled areas (from 3rd Bone Spring Sand to Wolfcamp-A2) almost immediately faded away as the pump shut off in the treatment well, whereas the strain signals in the shallower formations continued to extend upward. This observation indicates more mechanically induced strains from the 3rd Bone Spring Sand to Wolfcamp-A2, as they show a stronger correlation with hydraulic fracturing operations and actual fractures created.

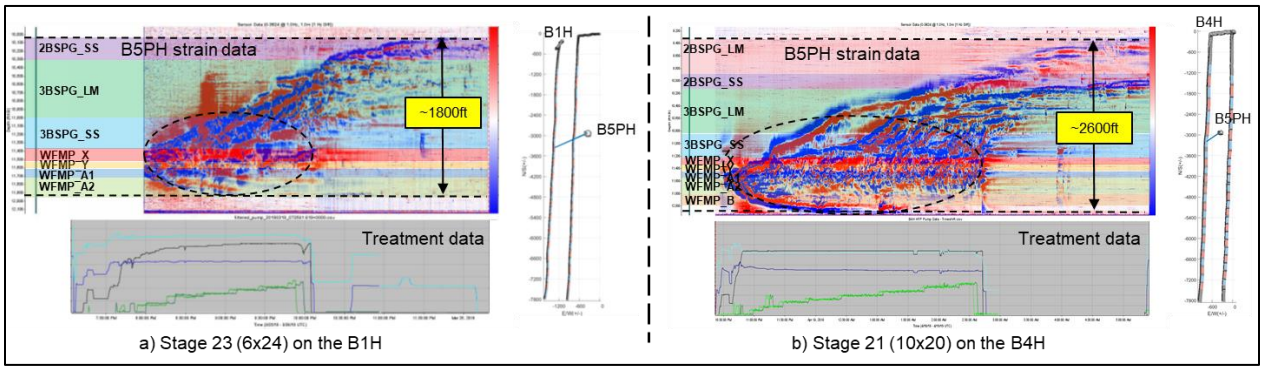

Figure 9. Strong far-field cross-well strain data acquired on B5PH during the treatment of Stage 23 (6×24) on the BX1H well (a) and Stage 21 (10×20) on the BX4H well (b)

FO-based MS monitoring was conducted in the HFTS-2 project, and the results were compared with conventional MS data. Some of the key insights from the FO interpretation include: fluid/proppant

Downloaded from http://onepetro.org/URTECONF/proceedings-pdf/21URTC/2-21URTC/D021S031R004/2477423/urtec-2021-5241-ms.pdf/1 by Carol Worster on 28 February 2022

allocation and evaluation of stimulation efficiency for different completion designs, observation of planar fracture propagation based on the far-field survey, and determination that the vertical propagation of hydraulic fractures from FO strain data should be an upper limit on fracture height and a data point for Shmax orientation. Only the highlights of the FO setup and far-field survey data interpretation are covered in this paper, but the insights on stimulation efficiency and completion designs comparison from analysis of near-wellbore survey data are covered in Zakhour et al., 2021.

Bottomhole Gauges

The pressures from bottomhole gauges were an important part of the HFTS-2dataset, quantifying the impact of frac hits and depletion. As many as 8 gauges on the vertical well (B5PH) and 12 gauges on the slant well (B6S) were installed spanning the formations from 3rd Bone Spring Sand to Wolfcamp-B. Each of child wells also had a bottomhole gauge. See Figure 10 for a pictorial representation of the gauges in relation to the child wells. The pressure data were analyzed during the stimulation of the child wells as well as during the production period.

<u>During Stimulation:</u>

The slant well was drilled after the stimulation of the child wells, so the vertical well gauges (8) along with the child well gauges were analyzed during the stimulation. As an example, the pressure change and pressure derivatives of the shallowest gauge are shown in Figure 10a during the stimulation of Stage 23 of well BX1H. The pressure derivative shows a strong inflection during the stimulation event. Analyzing all the gauges, we observe that the frac hit severity increases as we go to the shallowest gauge, indicating the preferential upward direction of fracture propagation (Figure 10b). Some of the other conclusions from the data are that all the child wells had frac hits on the gauges, the frac hits are perfectly aligned with the Shmax direction, and the existing gauge coverage isn't sufficient for fracture height estimation, as we see a response even in the shallowest gauge.

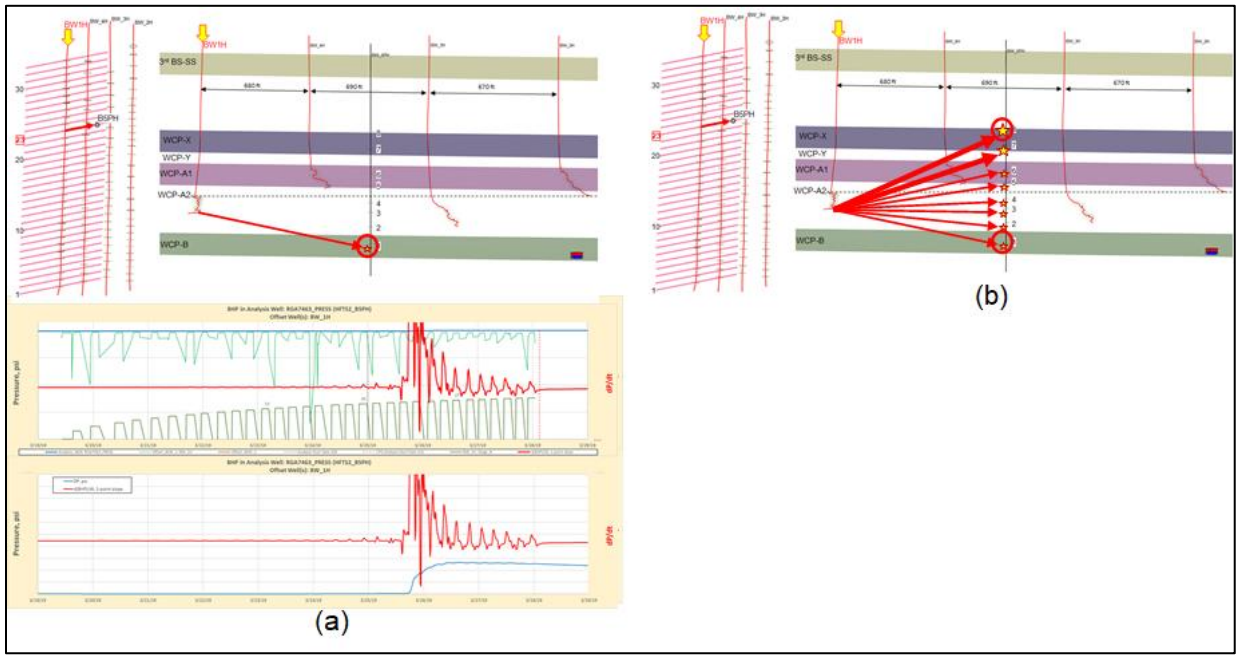

Figure 10. a) Pressure change (blue curve) and pressure derivative (red curve) in bottommost panel showing the impact of stimulation of Stage 23 in well BX1H on shallowest gauge in B5PH; b) Severity of frac hits decreases with depth in the vertical well gauges.

Downloaded from http://onepetro.org/URTECONF/proceedings-pdf/21URTC/2-21URTC/D021S031R004/2477423/urtec-2021-5241-ms.pdf/1 by Carol Worster on 28 February 2022

During Production:

The pressure drop seen in the gauges in vertical well B5PH show the depletion in each of the benches except Wolfcamp-B (Figure 11), which is confirmed by other diagnostics that show that the fractures don't grow downward. Figure 12 shows that bottomhole pressures measured at the same time at similar depths in the vertical well (B5PH) and slant well (B6S) were similar, lending confidence to the measurements.

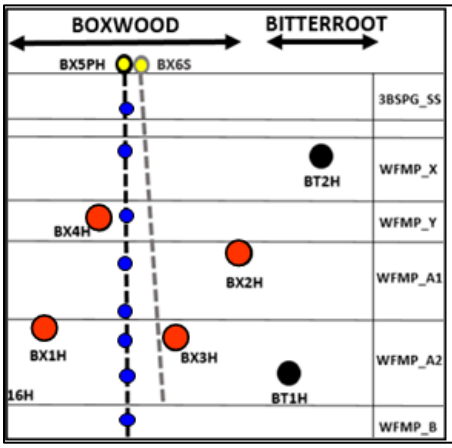

B5PH Gauge	Bench	6-month ΔBHP
1	BS3 (Shallowest)	-790 psi
2	WC-X	-763 psi
3	WC-Y	-632 psi
4	WC-A1	-470 psi
5	WC-A1	0 psi
6	WC-A2	-307psi
7	WC-A2	-307 psi
8	WC-B (Deepest)	0 psi

Figure 11. B5PH gauges pressure drop showing depletion in each bench

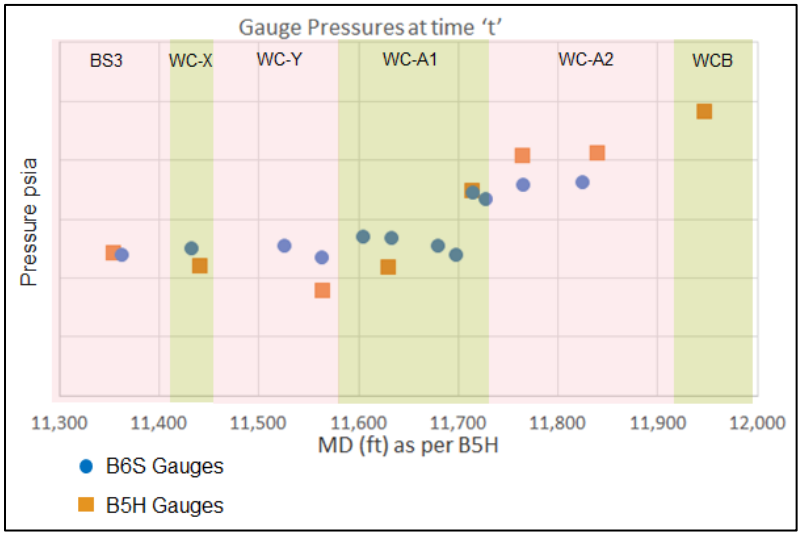

Figure 12. Bottomhole pressures in the vertical and slant well gauges

Well Interference Test Data

Two-well interference tests were conducted in the HFTS-2 area. In Feb. 2020, the first FO-based well interference and production logging test was designed and executed based on a proprietary procedure developed by ConocoPhillips (Jin et al., 2019). This test was conducted to identify flow connections between BX4H and the offset well, and to estimate the production log from the FO data for BX4H. After a long, stable production period and an 18-hour shut-in period, all involved wells in this test were cycled shut-in or open for shorter intervals of a few hours. Through analysis of the DAS data acquired on BX4H, no identifiable well interference between BX4H and the offset wells was observed, but the shut-in and open intervals (hours) were too short to record interpretable pressure gauge responses for analyzing communications between the child wells and the vertical or slant well. (See Figure 13)

Downloaded from http://onepetro.org/URTECONF/proceedings-pdf/21URTC/2-21URTC/D021S031R004/2477423/urtec-2021-5241-ms.pdf/1 by Carol Worster on 28 February 2022

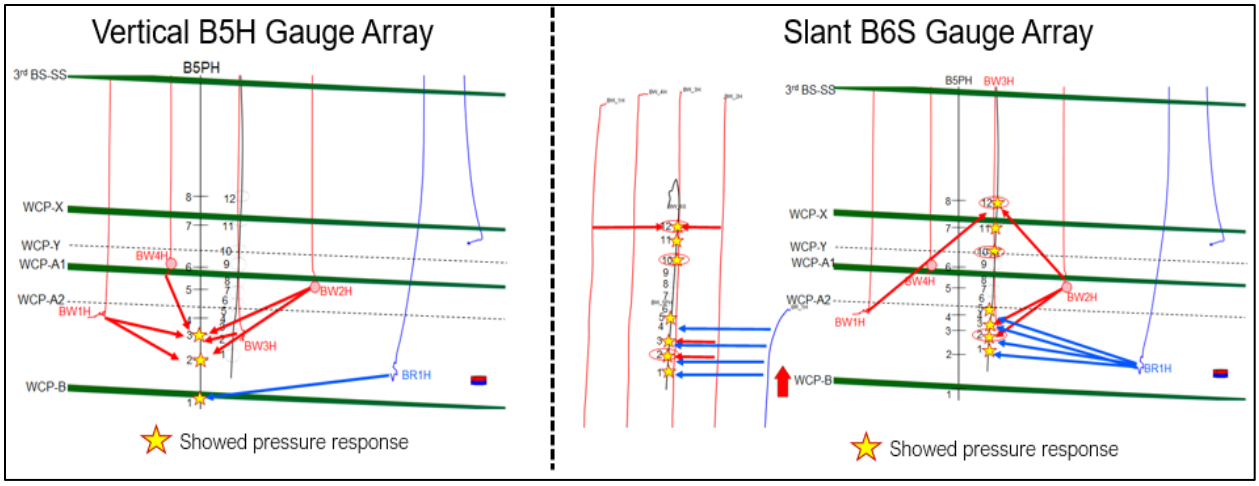

Figure 13. Pressure gauge responses during the FO-based interference test in Feb. 2020

The second test in Sept. 2020 was a dedicated pressure interference test with longer shut-in and open time intervals (3-6 days) on the two child wells, BX3H and BX4H. The longer durations allowed enough time for pressure signals to reach the offset wells and offered a better chance to confirm the well communications after 7 months of production. Figure 14 shows that the pressure response from shutting in and opening the BX3H and BX4H wells were picked up by four gauges in vertical well B5PH and 8 gauges in the slant well B6S. These signals enabled estimation of the SRV drainage height, which was 420 ft above the landing depth (Figure 14). The pressure signals at the gauges were weaker than the signals during the stimulation event. The drainage height estimated was compared with the other diagnostics during stimulation, but the pressure interference dataset differed from the diagnostics because the gauge signals (pressure depletion and derivatives) were a function of the overall drainage at that point in time and not the stimulation event. However, the drainage heights were in line with the estimations from completions and reservoir modeling, microseismic, and FO data.

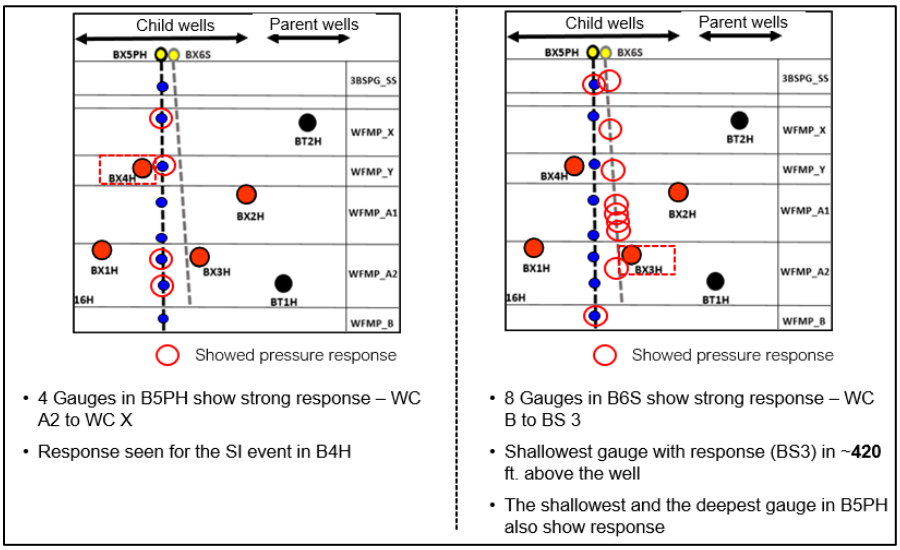

Figure 14. Pressure signal at the gauges during the dedicated Well Interference Test

During the two interference tests, DSS-RFS data were acquired on BX4H and showed encouraging potential for analyzing time-dependent fracture property changes in the near-wellbore region. The detailed interpretation and comparison with pumped fluid/proppant distribution among the clusters are covered in Zakhour et al., 2021.

Downloaded from http://onepetro.org/URTECONF/proceedings-pdf/21URTC/2-21URTC/D021S031R004/2477423/urtec-2021-5241-ms.pdf/1 by Carol Worster on 28 February 2022

Subsurface Models

Completions

All the child wells (BX1H–BX4H) were completed sequentially in a single well completion format. The completion designs were varied using Design of Experiments (DoE), which is discussed in detail in Zakhour et al., 2021. The extensive dataset of DFIT, falloff instantaneous shut-in pressure (ISIP), microseismic, image logs, and pressure interference were all available, so the completion modeling workflow had to be catered to include the essential elements. Modeling the impact of depletion from parent wells was critical to arriving at an accurate fracture geometry and characteristics in line with those obtained from diagnostics, which were only available for the child wells, not the parent wells. The first step of the workflow involved calibrating the non-depleted section of the child wells (North sector) to create an equivalent model for the parent wells. This intermediate step to create an updated stress map (pore pressure and Shmin) of the area enabled an accurate simulation of the subsequent child wells. These simulated child well fractures were then calibrated with the extensive diagnostics dataset. Due to the absence of zipper frac completion, intra-well stress shadowing was sufficient to improve the calibration process.

Simulation Modeling

Two approaches were employed for simulation modeling. The first was a traditional approach in which the model uses outputs from the completion models statistically along with in-house scripts for asymmetric fracture geometries and all the diagnostics data (FO, PIT, MS, BHPs) to match history. The second was a comprehensive geomechanics and flow simulation loop approach that couples and iterates between the geomechanics/completions models (GOHFER) and the dynamic simulation models (tNav) to incorporate the geomechanical stress shadowing. This approach takes more time to set up and run, but it provides an accurate understanding of the parent-child effects and helps optimize the stimulation design. The comprehensive modeling workflow for HFTS-2 is highlighted in the completions modeling section above.

Results and Discussion

Areal Coverage of Hydraulic Fractures

During Stimulation:

The comprehensive diagnostics dataset acquired during this project enabled the estimation of the hydraulic fracture dimensions. Figure 15 shows the areal coverage or length estimation of hydraulic fractures in four child wells from the various diagnostics and simulation results. The diagnostic-based (MS and FO) estimations for hydraulic fracture lengths (eastward and westward) are highlighted by the blue boxes, and the modeling-based results (fracture modeling from GOHFER and history-matched simulation) are highlighted by the red boxes. The results in Figure 15 are presented for the North sector (no depletion effects) and the South sector (strong parent-child effects), respectively.

Because BX2H is the closest child well to the two parent wells in the east, the fracture length results from diagnostics and simulations in the South sector show a significant eastward growth preference for the stages that overlap with the parent wells due to the strong depletion effect. This also aligns well with the identified hydraulic fractures of the parent wells from the interpretations of image log and proppant log data acquired on the BX2H well prior to stimulation (Figure 6). This eastward growth trend of hydraulic fractures was not observed for the stages of BX2H in the North sector. This critical observation is common to the BX1H, BX3H, and BX4H wells, which indicates the necessity of handling the North sector and South sector individually in the modeling efforts.

Downloaded from http://onepetro.org/URTECONF/proceedings-pdf/21URTC/2-21URTC/D021S031R004/2477423/urtec-2021-5241-ms.pdf/1 by Carol Worster on 28 February 2022

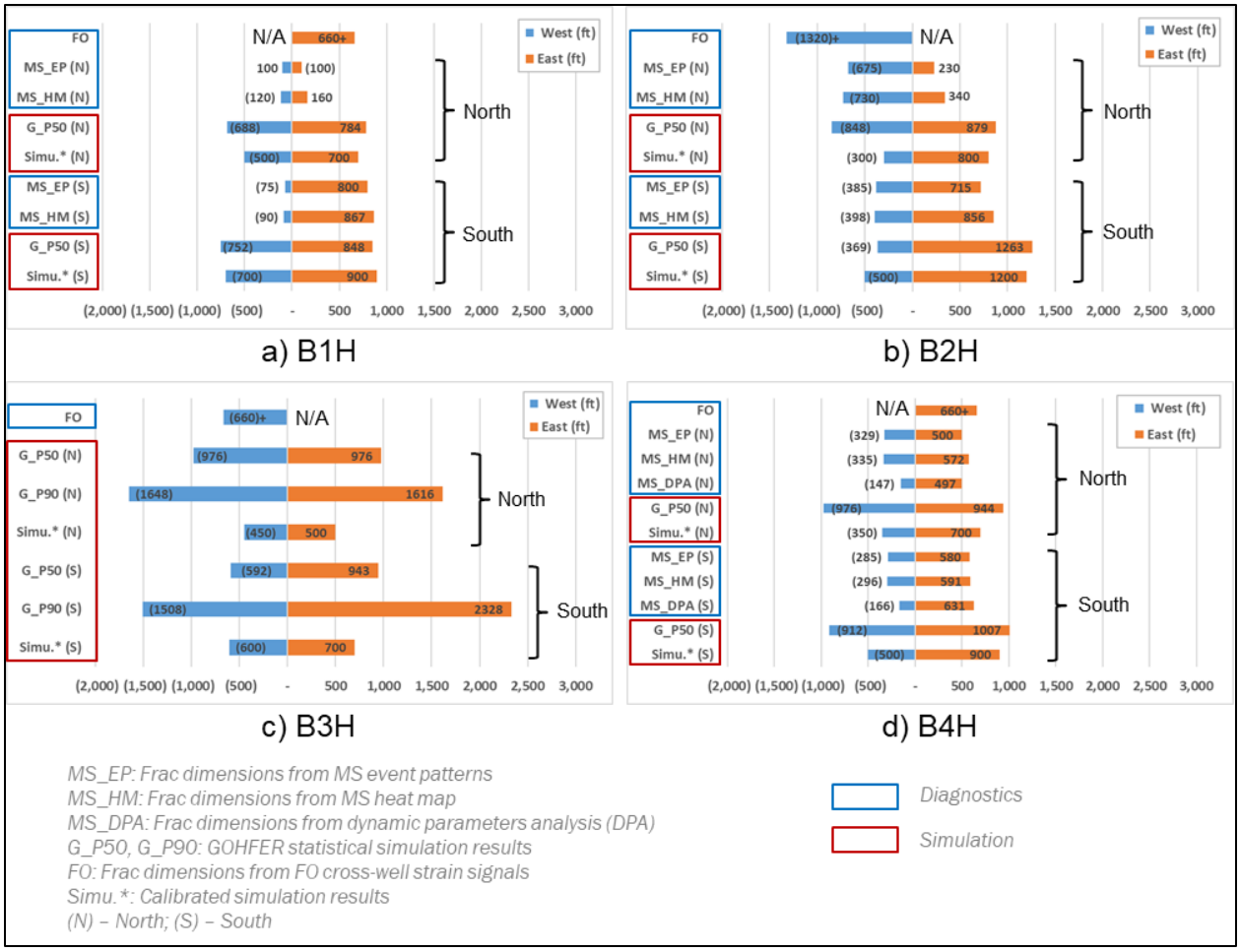

Figure 15. Areal coverage of hydraulic fractures in child wells from various diagnostics and simulation results

During Production:

Through comprehensive analysis of the acquired FO data along with pressure gauge responses, the two well interference tests did not show areal connections between child wells, but a few of the vertical and slant well pressure gauges picked up a clear signal response from the "shut-in" and "open" well events. The intensity of the pressure signal at the vertical and slant well gauges during production starts and stops appears to be weaker than that during the well stimulation phase.

The main implication of an asymmetric fracture from parent well influence will be on well spacing. The child wells need to be planned properly from a well placement and fracture sequencing perspective to maximize the new SRV formed by the fracturing process. If diagnostics are not available, sensitivities on fracture geometry asymmetry need to be considered.

Vertical Coverage of Hydraulic Fractures

During Stimulation:

Figure 16 shows the vertical coverage or height estimation of hydraulic fractures in the four child wells from various diagnostics and simulation results. All the child wells showed frac hits on the vertical well (B5PH), both from the pressure gauge responses (Figure 10) and far-field cross-well strain data. In terms of gauge response, the strongest effect was seen on the shallowest gauge located in the base of the 3rd Bone Spring formation, and the magnitude of the response decreased with depth towards the Wolfcamp-B formation. This observation indicates that the hydraulic fractures tend to grow upward during stimulation,

Downloaded from http://onepetro.org/URTECONF/proceedings-pdf/21URTC/2-21URTC/D021S031R004/2477423/urtec-2021-5241-ms.pdf/1 by Carol Worster on 28 February 2022

which is in good agreement with larger upward fracture height estimations from the various diagnostics. For both the North and South sectors, the microseismic-based fracture height estimations match well with the values from pressure gauge data and statistical GOHFER simulation results.

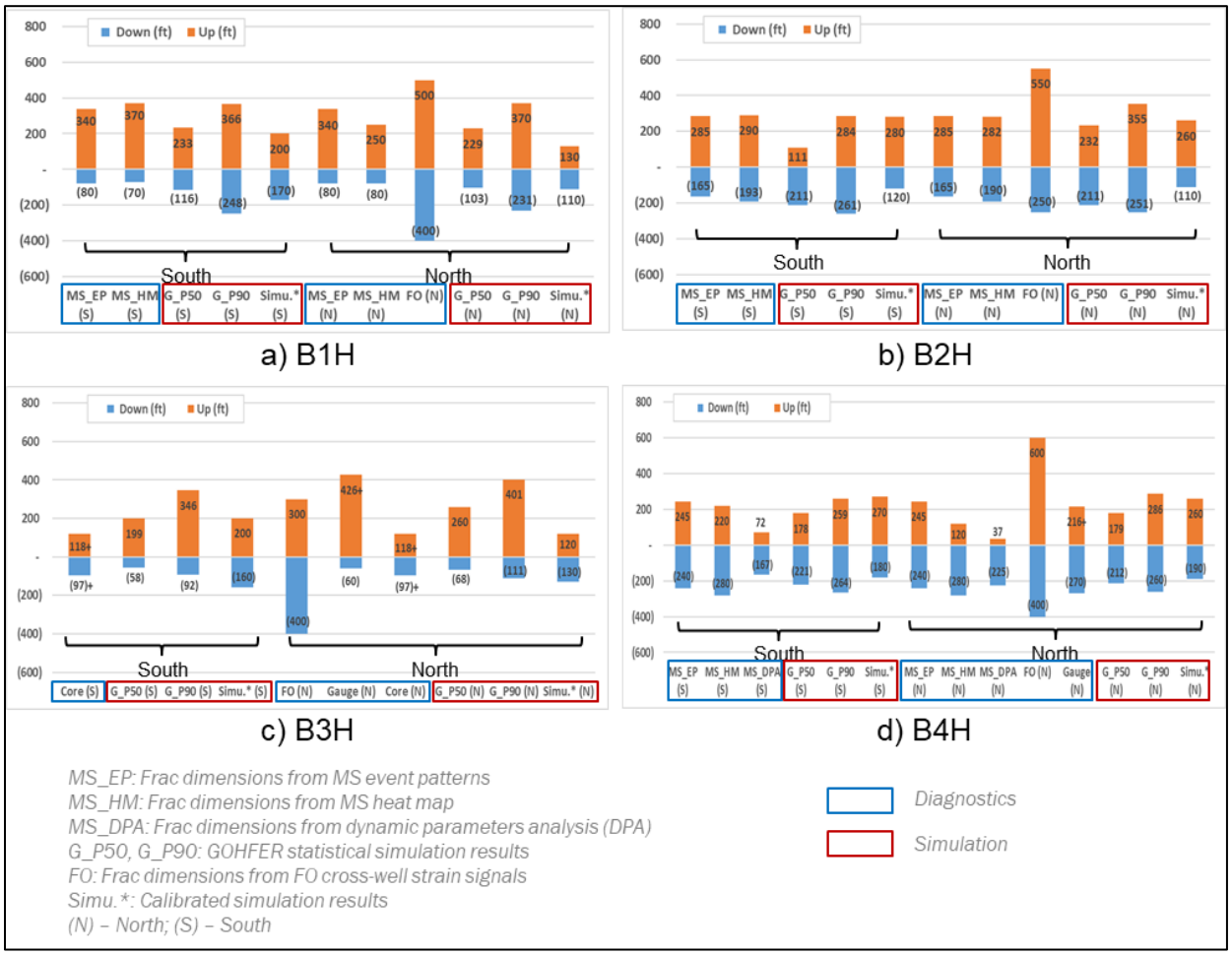

Figure 16. Vertical coverage of hydraulic fractures in child wells from various diagnostics and simulation results

In comparing different diagnostics, the fracture height estimations based on FO data always appear to be the upper bounds, which is due to the high sensitivity of FO to small strain changes that are not detectable by other diagnostics.

Figure 17 shows the integration of cross-well strain data on the B5PH well during the treatment of Stage 21 on BX4H with MS events distribution and pressure depletion profiles (at 1-, 2-, and 3-months of production) from 8 gauges on the B5PH well. The three panels share the same vertical depth axis. The stronger, mechanically induced strain signals in deeper formations are better correlated with MS events distribution (blue curve in the middle panel) for BX4H and the fracture height implication from pressure gauge data. A couple of points to note on the gauge data: 1) The height inference is based on production depletion and not stimulation, and 2) There are no gauges shallower than the 3rd Bone Spring, limiting the height inference to those benches.

Downloaded from http://onepetro.org/URTECONF/proceedings-pdf/21URTC/2-21URTC/D021S031R004/2477423/urtec-2021-5241-ms.pdf/1 by Carol Worster on 28 February 2022

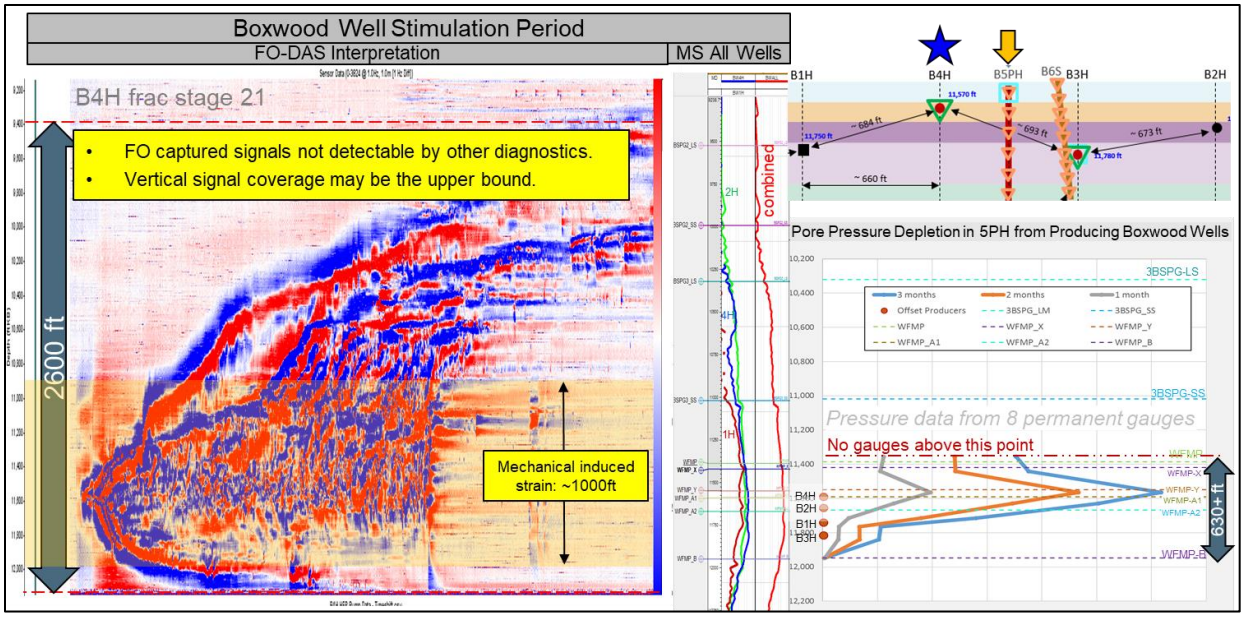

Figure 17. Integration of the FO vertical coverage data with microseismic and pressure gauge data

During Production:

A large pressure drawdown was observed all the way from the shallowest gauge in 3rd Bone Spring to the deeper gauges in Wolfcamp-A2 (Figure 11). Since there were no gauges installed on B5PH and B6S above the bottom of the 3rd Bone Spring formation, it was difficult to obtain pressure depletion information for shallower benches through conventional diagnostics. The FO along the wellbore of B5PH provides an alternative method to measure strain change as the proxy of vertical production depletion profile for all the wells. Figure 18 shows the strain change profiles acquired on the B5PH during the FO sensing test in Sept. 2020, when all the Boxwood wells were in a steady flow status before BX3H and BX4H were shut in. The strain measurement baseline in this test is very close to time stamp #1, as shown in Figure 18a, and therefore there is almost no strain change in all benches at time stamp #1 (Figure 18b). For time stamp #2 at the end of a steady flow period when there was about 45 psi BHP drawdown on BX4H, Figure 18c clearly shows strain depletion from the top of 3rd Bone Spring Sand to the middle of Wolfcamp-A2, whereas no strain depletion is evident in 3rd Bone Spring Lime and Wolfcamp-B. Since DSS-RFS is very sensitive to small rock deformation induced by pore pressure depletion, the strain change results during the steady flow period may provide a proxy of vertical production depletion profile from 3rd Bone Spring Sand to middle of Wolfcamp-A2 for all wells.

Downloaded from http://onepetro.org/URTECONF/proceedings-pdf/21URTC/2-21URTC/D021S031R004/2477423/urtec-2021-5241-ms.pdf/1 by Carol Worster on 28 February 2022

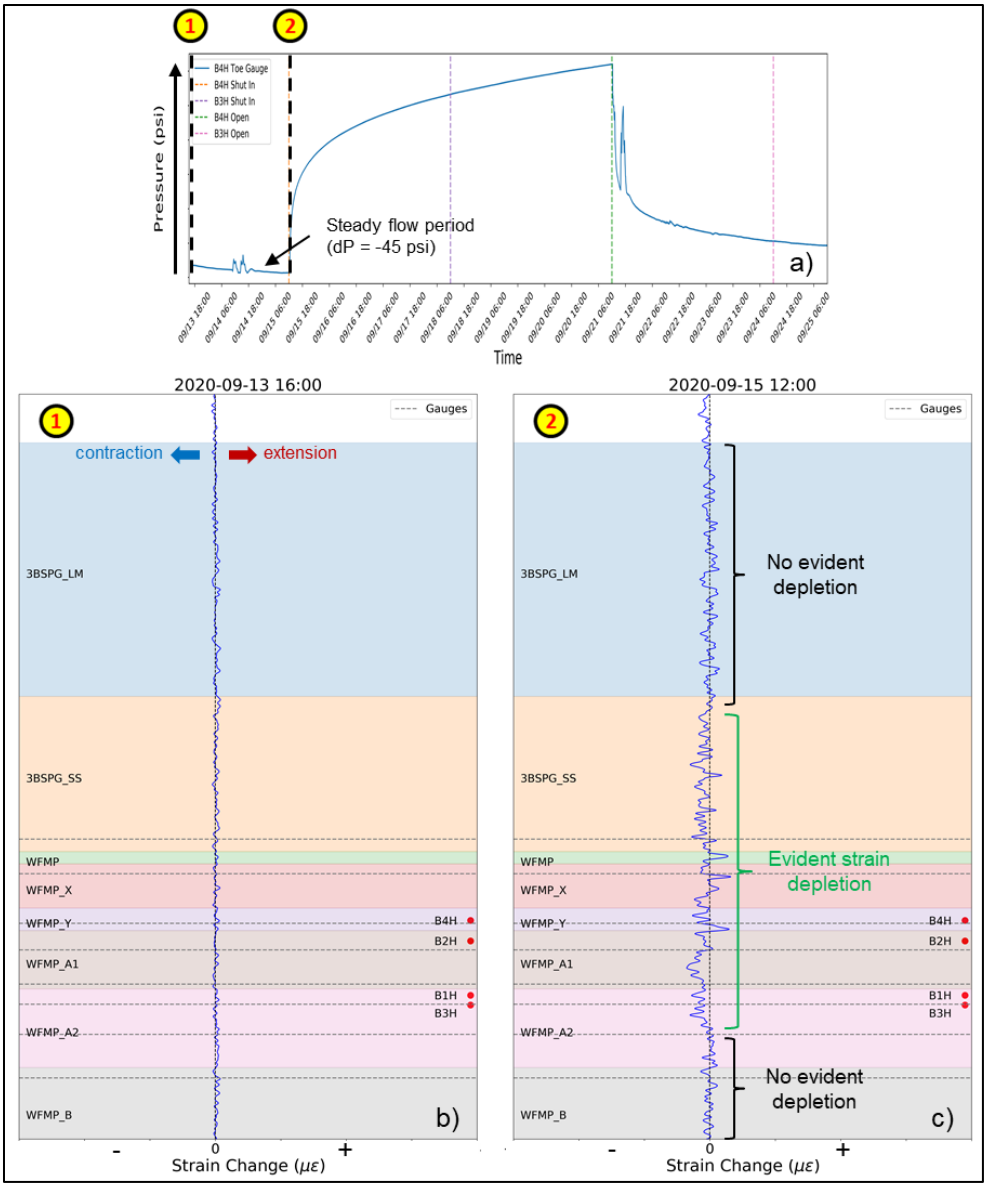

Figure 18. Strain change profiles during the steady flow period in the Sept. 2020 test. a) BX4H BHP change. b) Strain change profile at time stamp #1. c) Strain change profile at time stamp #2. Vertical dashed line at 0 indicates no strain change, and horizontal dash lines i and horizontal dash lines indicate locations of 8 P/T gauges on the B5PH. Red dots represent landing depth of four child wells.

Parent-Child Effects

The child well image logs serve as a good indicator for parent well HF tracking. The post-stimulation MS events have an eastward bias, in line with pre-stimulation image logs for stages that overlap parent wells (Figure 4, Figure 6). Figure 19 shows that during the child well stimulation (BX2H), tubing head pressures from the parent wells BR1H (blue curve) and BR2H (green curve) show strong frac hits. Even for the second offset child well (BX3H), which is 1,000–1,300 ft away from the parent wells, stimulation showed weak frac hits at the parent wells. In addition to the above diagnostics, calibrated subsurface models also showed a difference in geometries for stages affected by the depletion of parent wells.

The main implication of depletion (seen vertically) will be on co-development of multiple benches in a single section. Frac hits during stimulation of child wells show a pressure response, but a much stronger indication of effective drainage across all the formations of interest is the depletion seen during production. This depletion has strong implications on how these multiple formations can be co-developed.

Downloaded from http://onepetro.org/URTECONF/proceedings-pdf/21URTC/2-21URTC/D021S031R004/2477423/urtec-2021-5241-ms.pdf/1 by Carol Worster on 28 February 2022

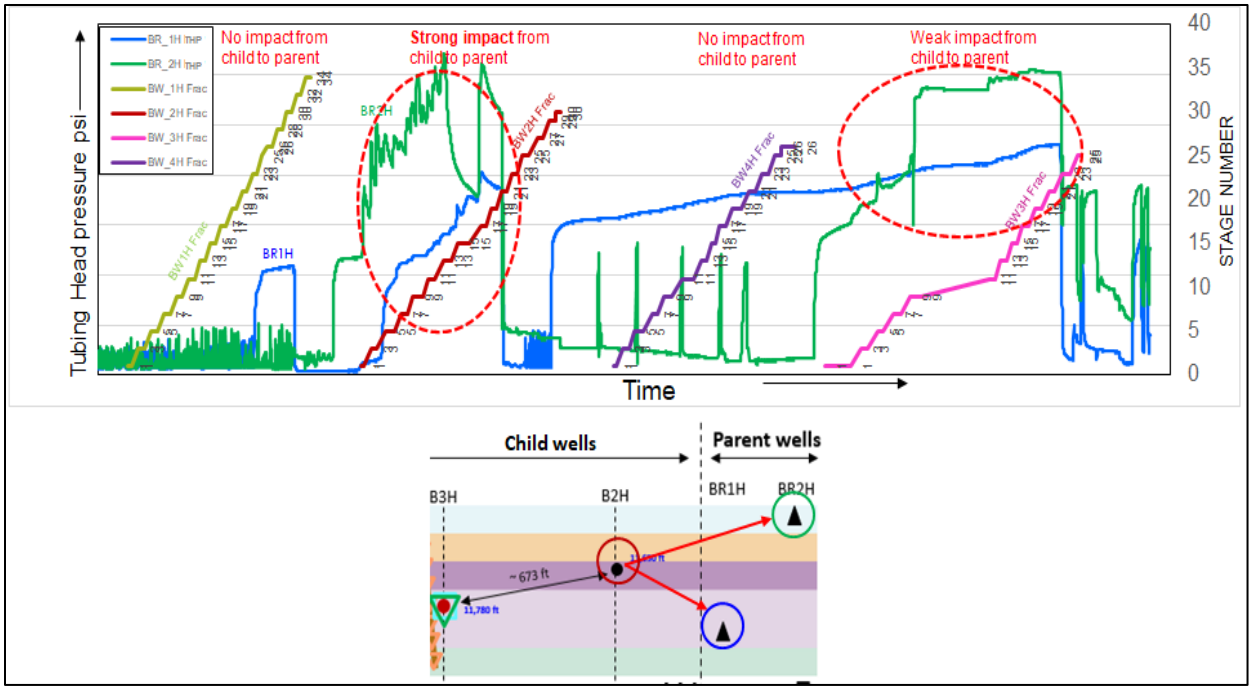

Figure 19. Top: Impact of child well stimulation (BX1H-BX4H) on the THP in parent wells (BR1H and BR2H); Bottom: Schematic showing the placement of the wells.

Conclusions

The comprehensive dataset acquired in HFTS-2 presents a unique opportunity to compare independent techniques to arrive at HF metrics (i.e., stimulation height and half-length) and quantify parent-child effects.

Areal Coverage: Conventional MS (and FO MS) were used to compute fracture half lengths, which were compared with diagnostics (FO strain, gauge, image logs), observations, and calibrated subsurface models. A post-production interference test did not show offset well communication, indicating that the pressure signals at the gauges were weaker than the signals during the stimulation event.

Vertical Coverage: Vertical coverage during stimulation was monitored using a vertical monitoring well. The stronger mechanical strain signals showed good correlation with MS event intensities, geomechanical properties, and gauge inferences. Vertical depletion was estimated based on vertical/slant well gauges, and strain depletion tests showed that the fiber-based height estimation was an upper bound on fracture height.

Parent-child effects: Diagnostics and calibrated subsurface models show asymmetry in child well fracture geometries for stages that overlap parent wells. Child well image logs serve as a good indicator for parent well HF tracking. Child well MS events had an eastward bias, in line with pre-stimulation image logs and confirmed by parent well frac hits.

Acknowledgments

The authors wish to thank the management of Occidental for permission to publish this paper. The authors would also like to acknowledge Jeanne Perdue for helping to edit this paper.

DOE acknowledgement: This material is based upon work supported by the Department of Energy under Award Number DE-FE0031577.

Disclaimer: "This report was prepared as an account of work sponsored by an agency of the United States Government. Neither the United States Government nor any agency thereof, nor any of their employees, makes any warranty, express or implied, or assumes any legal liability or responsibility for the accuracy, completeness, or

Downloaded from http://onepetro.org/URTECONF/proceedings-pdf/21URTC/2-21URTC/D021S031R004/2477423/urtec-2021-5241-ms.pdf/1 by Carol Worster on 28 February 2022

usefulness of any information, apparatus, product, or process disclosed, or represents that its use would not infringe privately owned rights. Reference herein to any specific commercial product, process, or service by trade name, trademark, manufacturer, or otherwise does not necessarily constitute or imply its endorsement, recommendation, or favoring by the United States Government or any agency thereof. The views and opinions of authors expressed herein do not necessarily state or reflect those of the United States Government or any agency thereof."

References

Bessa, F., Jerath, K., Ginn, C., Johnston, P., Zhao, Y., Brown, T., Lopez, R., Kessler, J., Nicklen, B., and Sahni, V. Subsurface Characterization of Hydraulic Fracture Test Site-2 (HFTS-2) Delaware Basin. Paper URTeC-5243 presented at the SPE/AAPG/SEG Unconventional Resources Technology Conference, Houston, Texas, USA, July 2021.

Grechka, V., Straus, C., Howell, B., and Furtado, D. Microseismic at HFTS-2: A story of three stimulated wells. Paper URTeC-5517 presented at the SPE/AAPG/SEG Unconventional Resources Technology Conference, Houston, Texas, USA, July 2021.

Jin, G., and Roy, B., 2017. Hydraulic-fracture geometry characterization using low-frequency DAS signal. *The Leading Edge*, v. 36, no. 12, pp. 975-980.

Jin, G., Friehauf, K., Roy, B., Constantine, J.J., Swan, H.W., Krueger, K.R., and Raterman, K.T. Fiber Optic Sensing-Based Production Logging Methods for Low-Rate Oil Producers. Paper URTeC-943 presented at the SPE/AAPG/SEG Unconventional Resources Technology Conference, Denver, Colorado, USA, July 2019. doi: https://doi.org/10.15530/urtec-2019-943.

Jin, G., Ugueto, G., Wojtaszek, M., Guzik, A., Jurick, D., and Kishida, K. Novel Near-Wellbore Fracture Diagnosis for Unconventional Wells Using High-Resolution Distributed Strain Sensing during Production. *SPEJ*. (2021). doi: https://doi.org/10.2118/205394-PA.

Maity, D. A Systematic Interpretation of Subsurface Proppant Concentration from Drilling Mud Returns: Case Study from Hydraulic Fracturing Test Site (HFTS-2) in Delaware Basin. Paper URTeC-5189 presented at the SPE/AAPG/SEG Unconventional Resources Technology Conference, Houston, Texas, USA, July 2021.

Molenaar, M.M., and Cox, B.E. Field Cases of Hydraulic Fracture Stimulation Diagnostics Using Fiber Optic Distributed Acoustic Sensing (DAS) Measurements and Analyses. Paper SPE-164030-MS presented at the SPE Unconventional Gas Conference and Exhibition, Muscat, Oman, January 2013. doi: https://doi.org/10.2118/164030-MS.

Ugueto, G.A., Todea, F., Daredia, T., Wojtaszek, M., Huckabee, P.T., Reynolds, A., Laing, C., and Chavarria, J.A. Can You Feel the Strain? DAS Strain Fronts for Fracture Geometry in the BC Montney, Groundbirch. Paper SPE-195943-MS presented at the SPE Annual Technical Conference and Exhibition, Calgary, Alberta, Canada, September 2019. doi: https://doi.org/10.2118/195943-MS.

Ugueto, G.A., Wojtaszek, M. A New Fracture Diagnostic Tool for Unconventionals High Resolution Distributed Strain Sensing via Rayleigh Frequency Shift during Production in Hydraulic Fracture Test 2. Paper URTeC-5396 presented at the SPE/AAPG/SEG Unconventional Resources Technology Conference, Houston, Texas, USA, July 2021.

Zakhour, N., Jones, M., Zhao, Y., Orsini, K., Sahni, V. HFTS-2 Completions Design and State-of-the-Art Diagnostics Results. Paper URTeC-5242 presented at the SPE/AAPG/SEG Unconventional Resources Technology Conference, Houston, Texas, USA, July 2021.

Downloaded from http://onepetro.org/URTECONF/proceedings-pdf/21URTC/2-21URTC/D021S031R004/2477423/urtec-2021-5241-ms.pdf/1 by Carol Worster on 28 February 2022